Quasiparticle Spectra, Charge-Density Waves, Superconductivity, and Electron-Phonon Coupling in 2H-NbSe$_2$

T. Valla,* A. V. Fedorov,† and P. D. Johnson

Department of Physics, Brookhaven National Laboratory, Upton, New York, 11973-5000, USA

P-A. Glans, C. McGuinness, and K. E. Smith

Department of Physics, Boston University, 590 Commonwealth Avenue, Boston, Massachusetts 02215, USA

E. Y. Andrei

Department of Physics, Rutgers University, 126 Frelinghuysen Road, Piscataway, New Jersey 08854, USA

H. Berger

Institute of Physics of Complex Matter, EPFL, Lausanne, Switzerland

High-resolution photoemission has been used to study the electronic structure of the charge-density wave (CDW) and superconducting dichalcogenide, 2H-NbSe$_2$. From the extracted self-energies, important components of the quasiparticle interactions have been identified. In contrast to previously studied TaSe$_2$, the CDW transition does not affect the electronic properties significantly. The electron-phonon coupling is identified as a dominant contribution to the quasiparticle self-energy and is shown to be very anisotropic (k dependent) and much stronger than in TaSe$_2$.

The family of layered 2H dichalcogenides represents an interesting system in which charge-density-wave (CDW) order coexists with superconductivity (SC) [1,2]. The CDW transition temperature decreases, while the superconducting critical temperature (T_C) increases from TaSe$_2$ through TaS$_2$ and NbSe$_2$ to NbS$_2$, suggesting that these two order parameters compete. Indeed, it has been found that, in TaS$_2$ and NbSe$_2$, T_C increases under pressure while T_{CDW} decreases [3,4]. After CDW order disappears, T_C remains approximately constant. In NbS$_2$, the system without CDW order, T_C is insensitive to pressure. Although various anomalies, including an apparent anisotropy of the superconducting gap, have been observed [5–8], it is generally believed that superconductivity in the dichalcogenides is of conventional BCS character, mediated by strong electron-phonon coupling [7]. However, consensus on the exact mechanism that drives the system into the CDW state has still not been reached. Some authors [1,2,9,10] argue that the CDW transition is driven by a Fermi surface (FS) instability (nesting), where some portions of the FS are spanned by a CDW vector—q_{CDW}. In another scenario, the CDW instability is induced by the nesting of van Hove singularities (saddle points in the band structure with a high density of states) if they are within a few $k_B T_{CDW}$ of the Fermi energy [11]. The Fermi surface of the 2H dichalcogenides is rather complicated, being dominated by several open (2D-like) sheets and with one small 3D S(Se)-derived pancakelike FS [7]. In such a situation, one may anticipate anisotropic properties and, in particular, an anisotropic electron-phonon coupling. The resistivity anisotropy, of the order of 10–50, is much smaller than in

layered oxides, indicating a substantial interlayer hopping [12]. Transport properties show relatively small anomalies at T_{CDW}, suggesting that only a small portion of the FS becomes gapped in the CDW state. In addition, the 2H dichalcogenides become better conducting in the CDW state, indicating a higher degree of coherence.

We have previously studied the quasiparticle (QP) self-energy for TaSe$_2$, and found that it was strongly influenced by the CDW transition [13]. The sharp structure in both the dispersion ("kink") and the scattering rate at ~70 meV in the CDW state weakened and shifted to ~35 meV upon transition to the normal state. Similar kinks have been previously identified in conventional metals and attributed to electron-phonon coupling [14]. As the energy scale of the kink in the CDW state of TaSe$_2$ was too large for phonons, we suggested that the excitation was electronic in origin: a fluctuation of the CDW order parameter. In this Letter, we show that the self-energy of NbSe$_2$ ($T_{CDW} \approx 35$ K and $T_C = 7.2$ K) is less sensitive to the CDW transition and that it is dominated by electron-phonon coupling. Measured directly for the first time, the coupling is very anisotropic, with the largest value on the inner K-H centered sheet.

The experiments reported here were carried out on a high-resolution photoemission facility based on undulator beam line U13UB at the National Synchrotron Light Source and a Scienta SES-200 electron spectrometer, which simultaneously collects a large angular window ≈14° of the emitted photoelectrons. The combined instrumental energy resolution was set to ~4 meV for low temperature studies ($T < 15$ K) and to ~6 meV elsewhere. The angular resolution was better than ±0.1° translating

into a momentum resolution of ± 0.0025 Å^{-1} at the 15.2 eV photon energy used. Samples, grown by the iodine vapor transport method, were mounted on a liquid He cryostat and cleaved *in situ* in the UHV chamber with base pressure 3×10^{-9} Pa. The temperature was measured using a calibrated silicon sensor mounted near the sample.

Figure 1 shows the photoemission intensity, recorded at $T = 10$ K, as a function of binding energy and momentum along three different momentum lines in the Brillouin zone. Nine Fermi crossings are included: three pairs on the double-layer split Fermi sheets centered around Γ and three crossings on the split sheets centered at the K point. A characteristic change in the QP velocity (kink) can be easily identified in all crossings. The kinks are also accompanied by a sharp change in the QP widths at the kink energy. These observations are indicative of (bosonic) excitations interacting with the QPs. The kink occurs roughly at the energy of the excitation involved in the coupling. Compared to TaSe$_2$, the excitation spectrum is limited to significantly lower energies. It also appears that the kink is not unique; its strength and energy depend on **k**, being different for different crossings. To quantify this, we have used momentum distribution curves (MDC) to extract the band dispersions for all the states shown. The dispersion curves provide direct information on the real part of the self-energy, ReΣ. As shown in the figure, the high energy part of the extracted dispersion can be fitted with a parabola that crosses through k_F, whereas the low energy part ($\omega < 15$–20 meV) is fitted with a straight line. If we assume that the parabola represents the "noninteracting" dispersion (i.e., the dispersion in the absence of interactions that cause the kink), then the slopes of these two lines at $\omega = 0$ may be used to directly extract the coupling constant, $\lambda = v_F^0/v_F - 1$, where v_F^0 is the noninteracting (bare) Fermi velocity and v_F is the renormalized one.

The noninteracting parabolas are further subtracted from the measured dispersions to extract Re$\Sigma(\omega)$. The

results are shown in Fig. 2(a) for several crossings from Fig. 1. Re$\Sigma(\omega)$ gives the same coupling constant ($\lambda = -[\partial(\text{Re}\Sigma)/\partial\omega]_0$), but also provides additional information about the spectrum of excitations interacting with the QPs. It is obvious from Fig. 2(a) that not only is the magnitude of ReΣ different for different states, but also the peaks are at different energies, ranging from $\sim$13 to $\sim$35 meV. Various experimental and theoretical studies have shown that the phonon spectrum is fully consistent with these energies, with acoustical branches laying below $\omega \sim 12$ meV, and optical branches spanning the region $15 < \omega < 40$ meV [15]. Shifts of the ReΣ maxima further suggest that some electronic states are coupled predominantly to acoustic modes while others couple more strongly to the optical modes, even though the states are sometimes very close in momentum (compare points 4 and 5, for example) [16]. It is interesting that in spite of these differences in Σ, the resulting coupling constant does not vary much, $\lambda \sim 0.85 \pm 0.15$, within the experimental uncertainty. The only exception is the inner K-centered sheet (point 6), where $\lambda \sim 1.9 \pm 0.2$. We have completed several measurements on different samples, always with similar results for λ at or close to that Fermi point. This seemingly too large coupling constant is actually in good agreement with the large measured value of linear specific heat coefficient, $\gamma \approx 18.5$ mJ mol^{-1} K^{-2} [5,17], which is proportional to the renormalized density of states (DOS) at the Fermi level, $N(0)(1 + \lambda)$, through $\gamma = (1/3)\pi^2 k_B^2 N(0)(1 + \lambda)$. Band structure calculations give the "bare" DOS $N(0) \sim 2.8$ states eV^{-1} unit cell^{-1} [7], suggesting $\lambda \sim 1.8$. However, even this might be an underestimate for our state as γ measures an average over the FS, weighted by each state's DOS. A similar value for λ is obtained from c-axis optical conductivity [18], suggesting that the c-axis transport is probably dominated by the K-H centered cylinders with the largest warping.

It is instructive that in TaSe$_2$ the CDW gap opens up in the same region of the FS [19], while the Γ-A centered
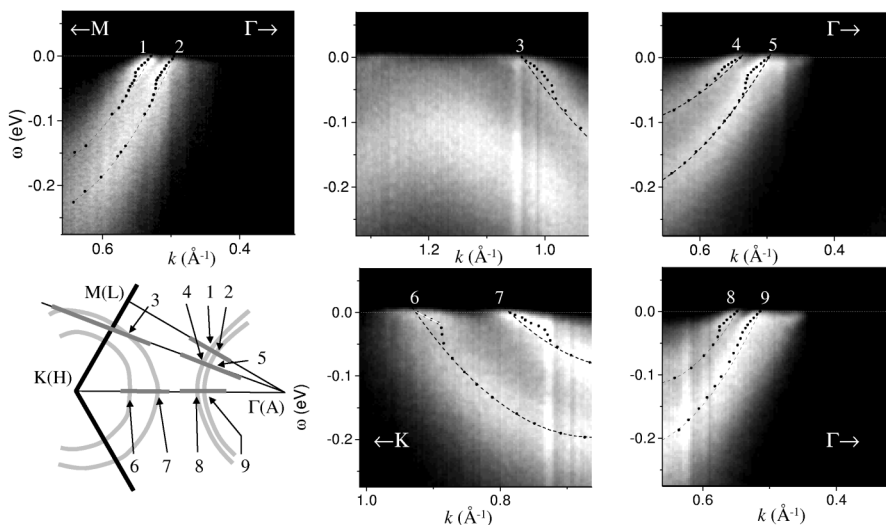

FIG. 1. The photoemission intensities in the CDW state at $T = 10$ K for several momentum lines indicated in the schematic view of the Brillouin zone (lower left panel) by the dark-gray lines. The light-gray lines represent Nb-derived Fermi sheets. The nine Fermi points are numbered. The MDC derived dispersions are represented by full circles. The high-energy part of the dispersions is fitted with a second-order polynomial (dashed lines), and the low energy part is fitted with straight lines.
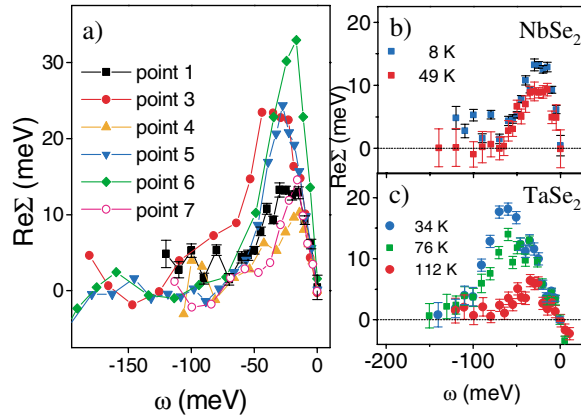
FIG. 2 (color). (a) Real parts of self-energies $Re\Sigma$ extracted from measured dispersions from Fig. 1 for several Fermi points. Temperature dependence of $Re\Sigma$ for (b) $NbSe_2$ for point 1 from Fig. 1 and for (c) $TaSe_2$ (taken from Ref. [13]) near the same region on the Γ-centered FS.

Fermi cylinders remain ungapped and gain coherence in the CDW state [13]. Therefore, it seems plausible that both the superconductivity and the CDW state originate from the inner K sheet and are driven by strong electron-phonon coupling. This seems to be in line with the original suggestion of Wilson [9] that the self-nesting of the inner K sheet drives the CDW in 2H dichalcogenides. A lack of CDW gap on the Γ centered sheets in all of 2H dichalcogenides studied in angle-resolved photoemission spectroscopy (ARPES) suggests that these sheets support neither the self-nesting nor the nesting which would mix them with the K-centered sheets. In particular, the f-wave symmetry of the CDW gap [2] may be ruled out. The relative strength of the CDW and superconducting ordering is determined by the nesting properties of the inner K cylinder, while the upper limit for T_C (when the CDW is destroyed by applying pressure, for example) is given by λ. Nesting weakens with increasing 3D character (increased warping with k_Z) under pressure and on moving from $TaSe_2$ to NbS_2. λ increases from $TaSe_2$ to $NbSe_2$ [20] and is essentially pressure independent. In agreement with previous ARPES studies [8,21,22], we do not see a CDW gap in $NbSe_2$, suggesting that the nested portion of the FS is very small and was not sampled in any study. As there is a nontrivial k_Z dispersion (warping), it is possible that the in-plane k_F might be tuned into the nesting and that the gap opens only near certain k_Z. Note that the energy splitting between the double walled sheets is larger for K-centered sheets. A similar k dependence is also expected for the interlayer hopping, $t_\perp$, that produces the warping. Additionally, as Fermi velocities are larger for Γ-centered sheets, it is reasonable to expect that the in-plane k_F varies with k_Z much less on the Γ cylinders than on the K cylinders (the change in the in-plane Fermi momentum is approximately given by $\Delta k_F \propto t_\perp / v_F$). The measured FSs centered at Γ are too large at the sampled k_Z, and we do not expect them to ever reach

the self-nesting condition $2k_F = q_{CDW}$. On the other hand, the inner K-centered sheet seems to be very close to producing the required nesting. A more detailed mapping is needed to explore the nesting properties and eventual CDW gap opening in this region. According to STM studies [23], the CDW gap is large ($\Delta_{CDW} \sim$ 35 meV) and should be easily measurable in ARPES. The overall electronic properties in $NbSe_2$ are much less sensitive to the CDW transition than in $TaSe_2$. Even the CDW induced structure in the self-energy that existed in $TaSe_2$ is absent in $NbSe_2$. Both the kink and the scattering rate are remarkably insensitive to the CDW [see Fig. 2(b)].

An interesting question is whether the anisotropic electron-phonon coupling constant λ would be projected into the magnitude of the superconducting gap. A recent photoemission study [8] has shown that the superconducting gap is indeed anisotropic, being quite uniform, $\Delta \sim$ 1 meV, on the Nb-derived Fermi cylinders, but reduced beyond the experimental sensitivity ($\Delta \approx 0$) on the 3D pancakelike FS. No data for the inner K-H cylinder have been reported. In Fig. 3 we show the spectral intensity at two Fermi points, 6 and 7, for several temperatures. The coupling constant differs by a factor of ~ 2 at these two points, and yet the superconducting gap (measured as the shift of the inflection point of the leading edge) that clearly opens up below T_C at both Fermi points is the same within the experimental error. This is in contrast to MgB_2, where the "hot" regions are gapped by correspondingly larger gaps [24]. The equalizing of the superconducting gap for states with different coupling strengths but similar symmetries represents a k space analogous to the proximity effect [25].

$NbSe_2$ has several properties in common with other layered materials. One of the most obvious peculiarities is the fact that the transport becomes more metallic in the CDW state even though a portion of the FS is "destroyed" (gapped). We suggest that this is a manifestation of anisotropic Fermi surfaces where strongly coupled portions, or "hot spots," generally play a negative role in normal state conductivities, acting as scattering "sinks" for the remaining, less renormalized regions. These hot spots drive the system into an ordered state, but it is the
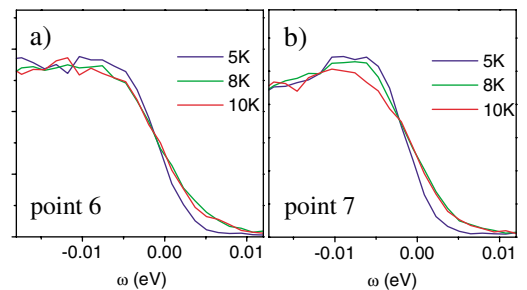

FIG. 3 (color). Temperature dependence of the EDCs at Fermi points of the inner (a) and the outer (b) Fermi sheets centered at K.

"cold spots" that usually dominate the conductivities. This duality has recently been detected in MgB_2 where the normal state transport shows an extremely weak coupling, while the superconducting properties are dictated by strongly coupled portions on the FS [24]. A similar situation also exists in the cuprates where the in-plane normal state properties are dominated by the near-nodal region [26]. The antinodal regions reduce the in-plane conductivities, while the opening of the pseudogap improves them.

Another similarity with the cuprates exists in that the pseudogap (T^*) and T_C lines in the T-x phase diagram of cuprates show similar behavior to the T_{CDW} and T_C lines in the T-pressure phase diagram of dichalcogenides. As $T^*(T_{CDW})$ goes down, T_C increases with doping (pressure). This analogy suggests that the cuprate phase diagram might be shaped by similar competing orders. However, the analogy is no longer valid in the overdoped regime where T_C turns back down, even when the pseudogap no longer exists, suggesting that some other, more exotic coupling mechanism might be acting in the cuprates. Here, we point out that the high energy of the kinks observed in $TaSe_2$ [13] and recently in $NbSe_3$ [27] rules out the phonon scenario and represents unambiguous evidence that the kinks may, indeed, be caused by other mechanisms. Consequently, the kinks observed in the cuprates [28] do not necessarily reflect the electron-phonon coupling.

In conclusion, we have detected a strong anisotropy of the self-energy in a layered dichalcogenide, $2H$-$NbSe_2$, with the electron-phonon coupling constant λ ranging from 0.8 to 1.9 on Nb-derived sheets. The strongest coupling has been found on the inner K-H cylinder, which plays a central role in both CDW and SC transitions in 2H dicalcogenides. The anisotropy in coupling strength does not induce the anisotropy in the SC gap.

*Electronic address: valla@bnl.gov
†Permanent address: Advanced Light Source, LBNL, Berkeley, CA 94720, USA.

[1] J. A. Wilson, F. J. Di Salvo, and S. Mahajan, Phys. Rev. Lett. **32**, 882 (1974).
[2] A. H. Castro Neto, Phys. Rev. Lett. **86**, 4382 (2001).
[3] F. Smith *et al.*, J. Phys. C **5**, L230 (1972); C. Berthier, P. Molinié, and D. Jérome, Solid State Commun. **18**, 1393 (1976); D. W. Murphy *et al.*, J. Chem. Phys. **62**, 967 (1975).
[4] P. Moline, D. Jérome, and A. J. Grant, Philos. Mag. **30**, 1091 (1974).
[5] P. Garoche *et al.*, Solid State Commun. **19**, 455 (1976); D. Sanchez *et al.*, Physica (Amsterdam) **204B**, 167 (1995).
[6] J. E. Graebner and M. Robbins, Phys. Rev. Lett. **36**, 422 (1976).
[7] R. Corcoran *et al.*, J. Phys. Condens. Matter **6**, 4479 (1994).
[8] T. Yokoya *et al.*, Science **294**, 2518 (2001); T. Kiss *et al.*, Physica (Amsterdam) **312–313B**, 666 (2002).
[9] J. A. Wilson, Phys. Rev. B **15**, 5748 (1977).
[10] N. J. Doran *et al.*, J. Phys. C **11**, 699 (1978).
[11] T. M. Rice and G. K. Scott, Phys. Rev. Lett. **35**, 120 (1975).
[12] B. Ruzicka *et al.*, Phys. Rev. Lett. **86**, 4136 (2001).
[13] T. Valla *et al.*, Phys. Rev. Lett. **85**, 4759 (2000).
[14] T. Valla, A. V. Fedorov, P. D. Johnson, and S. L. Hulbert, Phys. Rev. Lett. **83**, 2085 (1999); M. Hengsberger *et al.*, Phys. Rev. Lett. **83**, 592 (1999).
[15] J. L. Feldman, Phys. Rev. B **25**, 7132 (1982); G. Brusdeylins *et al.*, Phys. Rev. B **41**, 5707 (1990); Y. Nishio, J. Phys. Soc. Jpn. **63**, 223 (1994).
[16] A strong k dependence of Σ complicates the MDC line shape. However, we were not able to determine it precisely due to the overlap of bilayer split states.
[17] J. M. E. Harper, T. H. Geballe, and F. J. DiSalvo, Phys. Rev. B **15**, 2943 (1977); K. Noto, N. Kobayashi, and Y. Muto, Il Nuovo Cimento B **38**, 511 (1977).
[18] S. V. Dordevic, D. N. Basov, R. C. Dynes, and E. Bucher, Phys. Rev. B **64**, 161103 (2001).
[19] R. Liu *et al.*, Phys. Rev. B **61**, 5212 (2000); A. V. Fedorov *et al.* (unpublished).
[20] The $2H$-NbS_2 has slightly lower T_C ($\sim$6.3 K), suggesting a smaller coupling constant.
[21] Th. Straub *et al.*, Phys. Rev. Lett. **82**, 4504 (1999).
[22] W. C. Tonjes *et al.*, Phys. Rev. B **63**, 235101 (2001).
[23] H. F. Hess *et al.*, J. Vac. Sci. Technol. A **8**, 450 (1990).
[24] J. J. Tu *et al.*, Phys. Rev. Lett. **87**, 277001 (2001); H. J. Choi *et al.*, Nature (London) **418**, 758 (2002); H. J. Choi *et al.*, Phys. Rev. B **66**, 020513(R) (2002); S. Souma *et al.*, Nature (London) **423**, 65 (2003).
[25] H. Suhl, B. T. Matthias, and L. R. Walker, Phys. Rev. Lett. **3**, 552 (1959); M. E. Zhitomirsky and T. M. Rice, Phys. Rev. Lett. **87**, 057001 (2001).
[26] T. Valla *et al.*, Science **285**, 2110 (1999); T. Valla *et al.*, Phys. Rev. Lett. **85**, 828 (2000).
[27] J. Schäfer *et al.*, Phys. Rev. Lett. **91**, 066401 (2003).
[28] A. Lanzara *et al.*, Nature (London) **412**, 510 (2001); P. D. Johnson *et al.*, Phys. Rev. Lett. **87**, 177007 (2001).